Journal of Electrocardiology 77 (2023) 58–61

Contents lists available at ScienceDirect

Journal of Electrocardiology

journal homepage: www.jecgonline.com

Robustness of imageless electrocardiographic imaging against uncertainty in atrial morphology and location

Rubén Molero, Ana González-Ascaso, Andreu M. Climent [*,1], María S. Guillem [1]

ITACA Institute, Universitat Politècnica de València, València, Spain

ARTICLE INFO

Keywords:
Electrocardiographic imaging
Cardiac imaging
Imageless ECGI
Atrial location
Atrial morphology

ABSTRACT

Introduction: Electrocardiographic Imaging is a non-invasive technique that requires cardiac Imaging for the reconstruction of cardiac electrical activity. In this study, we explored imageless ECGI by quantifying the errors of using heart meshes with either an inaccurate location inside the thorax or an inaccurate geometry.
Methods: Multiple-lead body surface recordings of 25 atrial fibrillation (AF) patients were recorded. Cardiac atrial meshes were obtained by segmentation of medical images obtained for each patient. ECGI was computed with each patient's segmented atrial mesh and compared with the ECGI obtained under errors in the atrial mesh used for ECGI estimation. We modeled both the uncertainty in the location of the atria inside the thorax by artificially translating the atria inside the thorax and the geometry of the atrial mesh by using an atrial mesh in a reference database. ECGI signals obtained with the actual meshes and the translated or estimated meshes were compared in terms of their correlation coefficients, relative difference measurement star, and errors in the dominant frequency (DF) estimation in epicardial nodes.
Results: CC between ECGI signals obtained after translating the actual atrial meshes from the original position by 1 cm was above 0.97. CC between ECGIs obtained with patient specific atrial geometry and estimated atrial geometries was 0.93 ± 0.11. Mean errors in DF estimation using an estimated atrial mesh were 7.6 ± 5.9%.
Conclusion: Imageless ECGI can provide a robust estimation of cardiac electrophysiological parameters such as activation rates even during complex arrhythmias. Furthermore, it can allow more widespread use of ECGI in clinical practice.

Introduction

The standard ECG has not changed much in the last 80 years [1]. It has allowed the detection of many cardiac disorders but does not allow to infer of the cardiac activation pattern in each individual as an electroanatomical navigator does. A non-invasive visualization of cardiac electrical activity can be achieved, to a certain extent, through Electrocardiographic Imaging (ECGI) [2], which was validated in humans almost 20 years ago [3]. ECGI consists of estimating the electrical potentials on the surface of the cardiac chambers, from sets of 50 to 256 electrodes distributed over the torso of the patient [4,5].

ECGI has been demonstrated to be useful for mapping atrial flutters, characterizing AF, identifying extrasystole origin, or providing support during resynchronization pacemaker implantation [4–6]. During the last decade, commercial ECGI products have arrived on the market. Nevertheless, this novel non-invasive characterization tool of cardiac electrical activity has reached a moderate clinical impact. One potential reason for this limited clinical application of ECGI is the need for an accurate estimation of the torso and heart geometry from a CT scan of each patient while wearing the set of body surface electrodes. Potential complications associated with (1) a synchronization between cardiologists and radiologists and (2) irradiation into the patient for performing a CT scan to reconstruct the electrical activity are ethically justified only for a selected number of centers and patients.

The possibility of avoiding CT scans to perform ECGI maps is becoming an attractive approach to extend the advantages of a detailed non-invasive cardiac mapping to all cardiac arrhythmia patients [5,7]. Imageless ECGI allows estimating the cardiac geometry and its location inside the thorax of a patient based on a combination of statistical and electrical information, and thoracic geometrical information [7].

In this study, the robustness of our imageless ECGI is quantified. Specifically, the impact on ECGI signals of imposed geometrical

* Corresponding author at: ITACA Institute (COR), Universitat Politècnica de Valencia, Camino de Vera sn Ed. 8G, 46022 Valencia, Spain.
E-mail addresses: rumoal1@itaca.upv.es (R. Molero), acliment@itaca.upv.es (A.M. Climent), mguisan@itaca.upv.es (M.S. Guillem).
[1] Contributed equally to the supervision of the paper.

https://doi.org/10.1016/j.jelectrocard.2022.12.007

Available online 3 January 2023

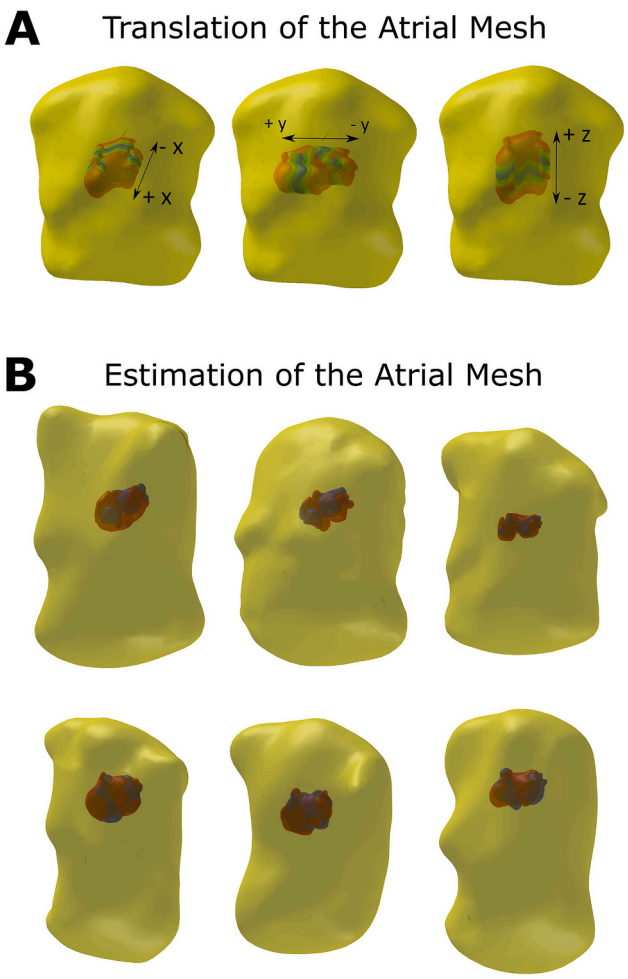

Fig. 1. Illustration of the geometrical distortions introduced in the performed experiments. In panel A, illustration of the translation of the atria inside the thorax of the patient along the X, Y, and Z axis, with maximal distances of 3 cm. In panel B, comparison between actual atrial mesh obtained from a CT scan atrium (red) and the estimated atrial geometry (blue) for 6 illustrative subjects. (For interpretation of the references to colour in this figure legend, the reader is referred to the web version of this article.)

distortions, modelling errors due to uncertainties in heart geometry, and location estimation is evaluated.

Material and methods

We recruited 25 patients referred for atrial fibrillation (AF) ablation at Hospital General Universitario Gregorio Marañón (Madrid, Spain). Institutional Ethics Committee approved the protocol, and all patients gave informed consent.

Fifty-seven body surface electrodes were distributed over the torso of each patient for the recording of ECGI signals. Signals were recorded at 1 kHz sampling rate with a bandpass filter between 0.05 and 500 Hz for off-line analysis. Surface signals were pre-processed as described in [8]. For each patient, a CT scan or MRI was acquired prior to the procedure to estimate the anatomy of the atria and the torso. In addition, 3D photogrammetry was used to reconstruct the torso of the patient and locate all ECGI electrodes. Torso and atrial geometries were co-registered using the torso reference from CT/MRI images [8].

To quantify the errors in ECGI reconstruction with estimated versus patient-specific atrial mesh, we used (1) different locations and (2) different morphologies of the atrial geometrical geometries together with the actual location and morphology of the atria of the patient and compared the estimated ECGI signals. The set of variations in the atrial mesh used for solving the inverse problem is summarized in Fig. 1. A set of displacements of 1, 2, and 3 cm in each axis (X, Y, and Z) was applied to all nodes of the CT/MRI derived atrial mesh of each patient (panel A). In addition, an estimated cardiac mesh, location, and rotation were obtained based on a statistical approach fed by the shape of the thorax of each patient (panel B) from a database of 30 atrial models. As it can be observed, the shape of the estimated and CT/MRI derived atria was different, but the location and mean size were similar.

Epicardial electrograms were then estimated from body surface recordings by using the boundary element method formulation and zero-order Tikhonov regularization and L-Curve selection of the optimal regularization parameter [9].

To compare electrograms estimated by solving the ECGI with the patient's CT/MRI derived atria versus the ECGI signals obtained with a different location or shape, we calculated Pearson's correlation coefficient (CC) and the relative difference measurement star (RDMS) [10] on each node of the atria. For comparison between ECGI signals obtained with different atrial geometries, the signals with pairing nodes were compared. For each node in the CT/MRI derived atrial anatomy, a pairing node was chosen for the estimated anatomy that minimized the Euclidean distance between these pairs of nodes. Pairs of nodes with distances larger than 0.5 cm were not used for comparison, using a total of 55.25 $\pm$ 14.15% of the nodes for the comparison Furthermore, to quantify the resemblance between the CT/MRI derived atrial geometry, the Hausdorff distance was computed between them as the longest distance between a node of a mesh and the closest node of the other.

In addition, dominant frequency (DF) maps were calculated from the ECGI signals obtained for translated and estimated atrial geometries and compared with the DF map obtained with the CT/MRI derived atrial geometry. DF was defined as the frequency with the largest power in the power spectral distribution obtained by applying the Welch periodogram (2-s Hamming window with a 25% overlap) [11]. The absolute difference in DF for each atrial node was quantified.

Results

Comparisons between ECGI signals are illustrated in Fig. 2. In panel A, the effects of the translation of the CT/MRI derived atrial mesh on the X, Y, and Z axis are depicted. As it can be observed, CC decreases with increasing translation distances while RDMS values were increased. Mean CC at a $\pm$ 1 cm translation was 0.98 $\pm$ 0.04 for the X axis, 0.98 $\pm$ 0.04 for the Y axis, and 0.97 $\pm$ 0.11 for the Z axis. The lowest correlations (0.82 $\pm$ 0.2) were found for translations of 3 cm on the X axis.

In panel B, an example of estimated ECGI signals obtained for CT/MRI derived versus estimated atrial geometries in a selected node is depicted. The correlation coefficient of both ECGI signals was 0.97, and the RDMS was 0.24. In panel C, the results for the entire database are depicted. The mean Hausdorff distance between the original and estimated geometries was 2.11 $\pm$ 0.66 cm. As it can be observed, by using the estimated geometry, an average correlation coefficient of 0.93 $\pm$ 0.11 and RDMS of 0.32 $\pm$ 0.18 were obtained.

DF maps obtained from ECGI signals estimated for the different atrial meshes (CT/MRI derived, translated, and estimated) are depicted in Fig. 3. In panel A, the DF map was measured by solving the ECGI with

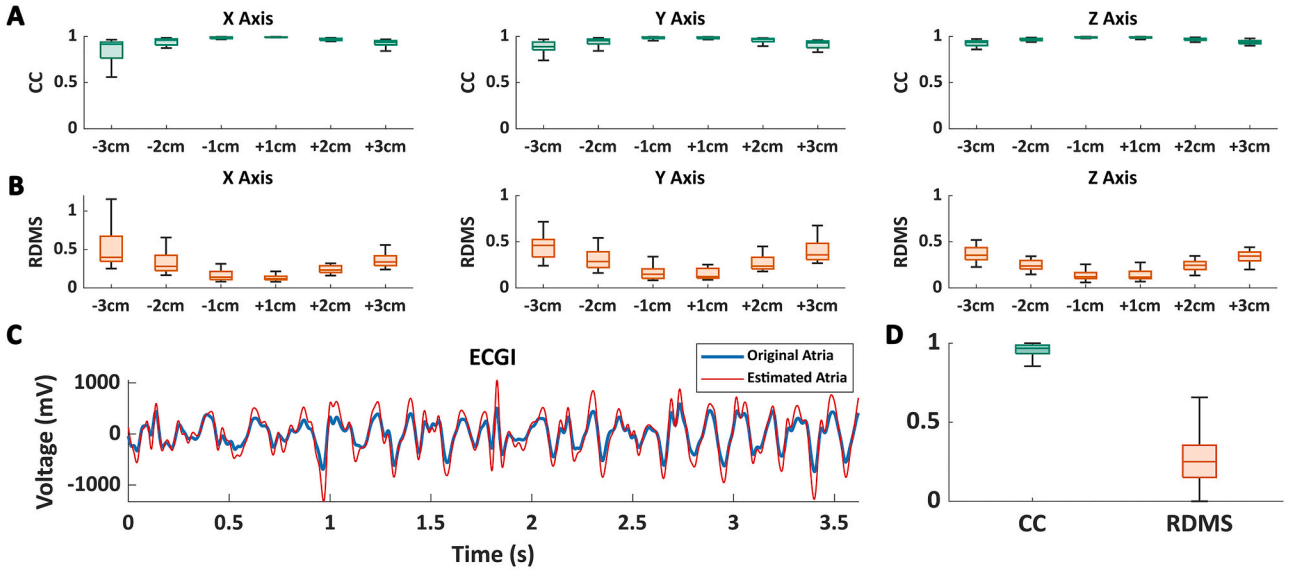

Fig. 2. Quantification of errors in ECGI signals by geometrical distortions. Panel A, CC, and RDMS obtained for translated atria in the X, Y, and Z axis by 1, 2, or 3 cm. Panel B, sample ECGI electrogram estimated for the CT/MRI derived atrial geometry of the patient (blue) together with the estimated ECGI signal at the nearest node for the estimated atrial geometry. Panel C, quantification of the Pearson's correlation coefficient (CC) and the relative difference measurement star (RDMS) between ECGI signals in all nodes in the actual atrial mesh obtained by a CT scan and pairing nodes in the estimated atrial meshes. (For interpretation of the references to colour in this figure legend, the reader is referred to the web version of this article.)

the CT/MRI derived patient anatomy derived from the CT scan or MRI. In this case, the highest DF (9.37 Hz) was present in the posterior side of the right atrium (RA), while most of the atria were activated at 4.82 Hz. In panel B, DF maps obtained with the original atrial geometry translated by ±1 cm in the X, Y, and Z axes are depicted. As it can be observed, DF maps were different when employing different atrial geometries, but the critical region, the site harboring the highest DF, was identifiable in all cases in the same region of the atria.

Finally, in panel C, the DF map obtained for the estimated cardiac geometry is depicted. Notice that although a few differences are noticeable between both maps, the values and distribution of DFs were correctly estimated. A systematic comparison between the DF values at all nodes and all patients obtained with the actual atrial geometry and the estimated geometry presented a mean difference of 0.47 ± 0.35 Hz.

Discussion

In this study, we have shown that an imageless ECGI allows to extract clinically relevant information without requiring a CT scan, even during complex arrhythmias such as AF.

Current non-invasive characterization of the cardiac function is insufficient for risk stratification or a personalized identification of the mechanisms maintaining arrhythmias in each individual patient. During the last decades, significant improvements have arrived at the clinic by the hand of image and structural analysis developments thanks to systems such as echocardiography, CT scans, and MRI. However, regarding the electrophysiological function of the heart, main technological novelties have been restricted to the improvement of invasive electroanatomic mapping systems. Non-invasive characterization continues to be limited to the standard ECG used without major developments during the last century. ECGI could fill the gap between the ECG and electroanatomical mapping. However, the introduction of current ECGI technology in clinical practice is hampered because of the extra efforts that need to be put into the acquisition of a CT scan of the patient while wearing a multielectrode vest. Primary and secondary patient care could also take advantage of imageless ECGI solutions since this non-invasive characterization could help predict the optimal treatment on an individual patient basis without requiring a CT scan or MRI in each patient. Development of imageless ECGI, together with a reduction of the number of leads needed [12,13] and the optimization of the regularization process to increase accuracy [10], is the way to follow in order to extend the applicability of this technology. In addition, the combination of apriorism knowledge and mathematical electrophysiological models offers a promising line of research [14,15].

In the present study, we have evaluated the effect of uncertainty on atrial geometry estimation during AF episodes since this could be considered a worst-case scenario with low signal-to-noise ratios and high variability in the ECG signals. In addition, although AF is the most prevalent arrhythmia, current characterization based on the standard ECG is insufficient to select the best treatment for each patient. Extension of the present results to the characterization of more regular rhythms or ventricular arrhythmias will help to validate the application of imageless ECGI. It is remarkable to notice that the estimation of cardiac chambers is based on previous knowledge and extensive databases of patients, but in case of congenital or significant heart disease that could imply dramatic changes in the cardiac morphology would continue requiring a CT scan.

Conclusion

Imageless ECGI can provide a robust estimation of cardiac electrophysiological parameters such as activation rates even during complex arrhythmias such as AF. Estimation of a patient's cardiac geometry and its most plausible location inside the thorax opens the possibility of helping the application of non-invasive electrophysiological maps in clinical practice.

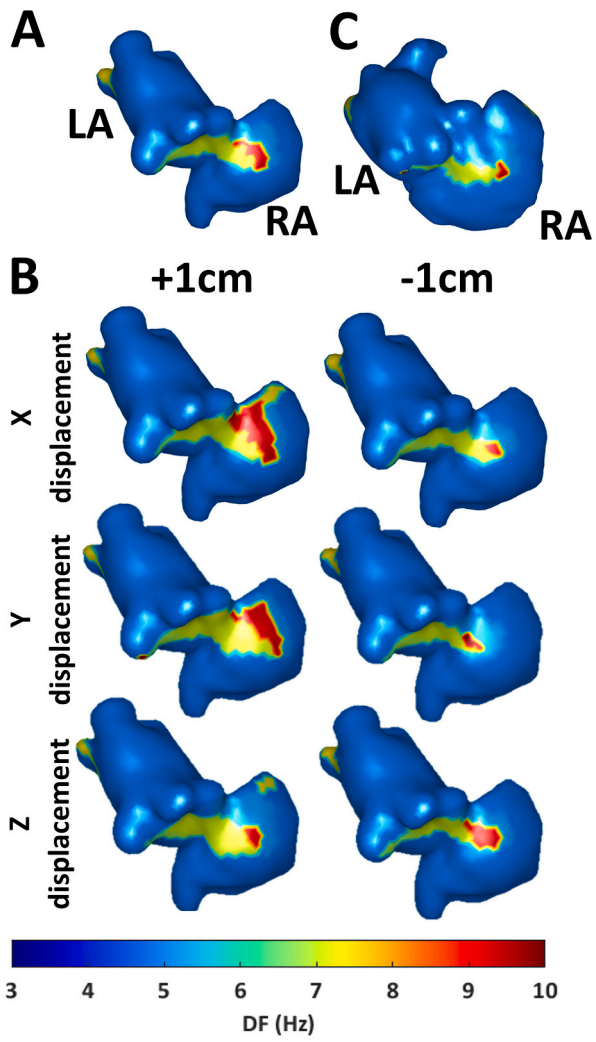

Fig. 3. Effects of geometry and location errors on atrial fibrillation DF maps. Panel A. DF map obtained from ECGI signals estimated for the patient's CT/MRI derived atrial mesh. Panel B, effects of the translation of the patient's CT/MRI derived atrial mesh along the X, Y, and Z axis on the DF map. Panel C. DF map obtained from ECGI signals computed for an estimated atrial mesh.

Disclosures

MS Guillem and AM Climent are co-founders and shareholders of Corify Care SL.

Author statement

R. Molero contributed to the experimentation and design of the figures and final manuscript.

A. González-Ascaso contributed to the experimentation of the study.

MS Guillem and AM Climent contributed equally to the design of the experiments and final manuscript.

Declaration of Competing Interest

R. Molero and A. González-Ascaso have no conflict of interests.

Acknowledgments

This work was supported by: Instituto de Salud Carlos III, and Ministerio de Ciencia e Innovación (supported by FEDER Fondo Europeo de Desarrollo Regional DIDIMO PLEC2021-007614, ESSENCE PID2020-119364RB-I00, and RYC2018-024346-I), EIT Health (Activity code SAVE-COR 220385, EIT Health is supported by EIT, a body of the European Union) and Generalitat Valenciana Conselleria d'Educació, Investigació, Cultura i Esport (ACIF/2020/265). The authors want to thank the organizers of the 2022 meeting of the International Society for Computerized Electrocardiology for their invitation to the meeting.

References

[1] Goldberger E. A simple, indifferent, electrocardiographic electrode of zero potential and a technique of obtaining augmented, unipolar, extremity leads. Am Heart J 1942;23:483–92. https://doi.org/10.1016/S0002-8703(42)90293-X.

[2] Barr RC, Spach MS. Inverse calculation of QRS-T epicardial potentials from body surface potential distributions for normal and ectopic beats in the intact dog. Circ Res 1978;42:661–75. https://doi.org/10.1161/01.RES.42.5.661.

[3] Ramanathan C, Ghanem RN, Jia P, Ryu K, Rudy Y. Noninvasive electrocardiographic imaging for cardiac electrophysiology and arrhythmia. Nat Med 2004;10:422–8. https://doi.org/10.1038/nm1011.

[4] Cluitmans M, Brooks DH, MacLeod R, Dössel O, Guillem MS, Van Dam PM, et al. Validation and opportunities of electrocardiographic imaging: from technical achievements to clinical applications. Front Physiol 2018;9:1–19. https://doi.org/10.3389/fphys.2018.01305.

[5] Salinet J, Molero R, Schlindwein FS, Karel J, Rodrigo M, Rojo-Álvarez JL, et al. Electrocardiographic imaging for atrial fibrillation: a perspective from computer models and animal experiments to clinical value. Front Physiol 2021;12:1–23. https://doi.org/10.3389/fphys.2021.653013.

[6] Bear LR, Bouhamama O, Cluitmans M, Duchateau J, Walton RD, Abell E, et al. Advantages and pitfalls of noninvasive electrocardiographic imaging. J Electrocardiol 2019;57:S15–20. https://doi.org/10.1016/j.jelectrocard.2019.08.007.

[7] Rodrigo M, Guillem MS, Climent AM, Liberos A, Hernández-Romero I, Arenal Á, et al. Solving inaccuracies in anatomical models for electrocardiographic inverse problem resolution by maximizing reconstruction quality. IEEE Trans Med Imaging 2018;37:733–40. https://doi.org/10.1109/TMI.2017.2707413.

[8] Molero R, Soler Torro JM, Martínez Alzamora N, M. Climent A, Guillem MS.. Higher reproducibility of phase derived metrics from electrocardiographic imaging during atrial fibrillation in patients remaining in sinus rhythm after pulmonary vein isolation. Comput Biol Med 2021;139:104934. https://doi.org/10.1016/j.compbiomed.2021.104934.

[9] Pedrón-Torrecilla J, Rodrigo M, Climent AM, Liberos A, Pérez-David E, Bermejo J, et al. Noninvasive estimation of epicardial dominant high-frequency regions during atrial fibrillation. J Cardiovasc Electrophysiol 2016;27:435–42. https://doi.org/10.1111/jce.12931.

[10] Figuera C, Suárez-Gutiérrez V, Hernández-Romero I, Rodrigo M, Liberos A, Atienza F, et al. Regularization techniques for ECG imaging during atrial fibrillation: A computational study. Front Physiol 2016:7. https://doi.org/10.3389/fphys.2016.00466.

[11] Rodrigo M, Climent AM, Liberos A, Fernández-Avilés F, Berenfeld O, Atienza F, et al. Highest dominant frequency and rotor positions are robust markers of driver location during noninvasive mapping of atrial fibrillation: A computational study. Heart Rhythm 2017;14:1224–33. https://doi.org/10.1016/j.hrthm.2017.04.017.

[12] Guillem MS, Bollmann A, Climent AM, Husser D, Millet-Roig J, Castells F. How many leads are necessary for a reliable reconstruction of surface potentials during atrial fibrillation? IEEE Trans Inf Technol Biomed 2009;13:330–40. https://doi.org/10.1109/TITB.2008.2011894.

[13] Parreira L, Carmo P, Adragao P, Nunes S, Soares A, Marinheiro R, et al. Electrocardiographic imaging (ECGI): what is the minimal number of leads needed to obtain a good spatial resolution? J Electrocardiol 2020;62:86–93. https://doi.org/10.1016/j.jelectrocard.2020.07.004.

[14] van Dam PM. A new anatomical view on the vector cardiogram: the mean temporal-spatial isochrones. J Electrocardiol 2017;50:732–8. https://doi.org/10.1016/J.JELECTROCARD.2017.08.010.

[15] Van Oosterom A. ECGSIM: an interactive tool for studying the genesis of QRST waveforms. Heart 2004;90:165–8. https://doi.org/10.1136/hrt.2003.014662.